AMARADAR-1 Project Journal

Leonard K. McGuire Jr.
March 25, 2016

Abstract

This journal covers the findings from work on the project AMARADAR-1. The goals of the project are high resolution with low power radar mapping experimentation. The test equipment consists of a USRP B200, parabolic dish, and feed horn. The journal involves various experimentation and findings of an amateur level in radar. This journal is expected to serve as a reference. The mapping involves atmospheric phenomenon, weather, structures, and ground penetration.

> "His invisible attribute are clearly seen, being understood by the things that are made, even His eternal power and Godhead, so that they are without excuse, ..."
>
> Romans 1:20, NKJV

Contents

Definitions & Equipment

The test is conducted using one USRP B200, one indiscernible horn feed antenna from a discarded parabolic reflector, and a 3-meter fiberglass parabolic reflector. Some primitive testing indicates that the horn feed antenna performs well in the range of 1.2GHZ to 3.0GHZ. In these tests USB 2.0 was recommend to use an external AC/DC power input to the USRP B200 but this was not available, therefore, only USB 2.0 power was supplied to the USRP B200.

RX means receiver channel and TX means transmit channel. RXB denotes a specific receiver channel or RX/TX may denote a specific channel used for both.

The dBm is used as:
$dbm = 10 * log(1000 * watt, 10)$
$watt = 10^{(dbm/10)/1000}$.

The dB for gain is as:
$dB = 20 * log(gain, 10)$
$gain = 10^{dB/20}$

The dBm[fft:x] is defined as the dBm function of the FFT magnitude output using an FFT bucket count of x.

The USRP B200 is specified as having a maximum specification of -15dBm for RX and the card generally returns complex samples with a magnitude less than 1.41, therefore, it is correlated without great confidence that -15dBm is 1.41 in magnitude. The following formula is used to exchange between power and magnitude considering RX gain.
$magnitude_{real} = magnitude_{input}/10^{dB/20}$

This gives the ability to transfer complex sample magnitude with RX gain into wattage and decibel.

1 Session 031916

Test Parameters

The tests were conducted at 1.26GHZ. The sky was cloudy with light rain earlier in the day; however, at the time of test there was no rain. The wind during the test was in gusts of 10MPH. The time was 1600 CDT on March 19th, 2016. The transmitter and receiver are not ensured to have started at the same time. The transmitter and receiver both shared the same antenna port in half-duplex mode. The receiver was switched out by the hardware when the transmitter was activated and switched back in via an electronic switch on the board. The TX gain was 60dB and the RX gain was 73dB.

1.1 TX-2MSPS-10TICKS.RX-8MSPS-1K6K-30KTICKS-0319161400

These tests transmitted two signals at one kilohertz and six kilohertz positive offset from a center frequency of 1.26GHZ using I/Q generated samples send to a transmitter at 2MSPS for a length of 10 samples. The receiver was on for 30000 samples at 8MSPS. This was repeated 6 times.

1.1.1 RUN-01

Small background noise up until sample 9344 which was the start of a high energy wide band burst that lasted less than 128 samples. Afterwards, the data was oddly at absolute zero. A closer inspection revealed that the burst consisted of an abnormal high deflection of both the I and Q components for 6 samples in the negative direction.

The cause and meaning are not understood of the burst and sudden silence. It could be possible that the card buffer was under or over run; however, that would not explain the high deflection.

1.2 RUN-02

A FFT of 15360 buckets on the 8MSPS stream shows a concentration of energy with in 4KHZ of center and then a second high concentration at about 5.04KHZ with both 15360 samples long; however, closer inspection reveals the energy last a shorter amount of time. As the FFT bucket size is decreased the energy concentration remains and shows decay. With an FFT size of 4 there is significant energy at sample 12 to sample 16 with a 5dBm drop on both sides. From there on periodic energy concentrations exist that primarily decay with intermediate increases. Most are 2dB pulses but also found after those, being the intermediate increases, are 4dBm which are almost in magnitude of a pulse to compare to the original first pulse. At 4148 there exists only one more significant pulse at 5840 then the energy remains similar to that outside of the center FFT bin. There are sporadic looking impulses existing in the two immediate buckets both negative and positive offset but very few but of 2dBm in strength.

start	length	magnitude	feet
68	500 nsecs	3.9dBm[fft4]	960ft
104	500 nsecs	3.9dBm[fft4]	3120ft
132	500 nsecs	4.77dBm[fft4]	4800ft
160	500 nsecs	3.9dBm[fft4]	6480ft
176	1000 nsecs	6dBm[fft4]	7440ft
228	500 nsecs	5.44dBm[fft4]	10560ft
256	500 nsecs	3.97dBm[fft4]	12240ft
292	500 nsecs	7.16dBm[fft4]	14400ft

Table 1: TX-2MSPS-10TICKS.RX-8MSPS-1K6K-30KTICKS-0319161400-RUN02

The TX channel should have only produced 10 samples and then become inactive. Since the TX channel operated at 2MSPS this would have been equivalent to 40 samples on the RX channel. Since neither the RX or TX is confidently synchronized in starting time it is plausible to not see the impulse or for the impulse to start anywhere after the first RX sample; however, the TX impulse should only be 40 samples.

The dBm figures do not compensate for RX gain, but use the magnitude of the FFT output.

If the TX impulse is considered starting at sample 12 then it should end at about sample 52. This leaves the next major impulses to be at samples 180(6.4dBm[fft4] 1usec), 228(6.0dBm[fft4] 0.5usec), 288(6dBm[fft4] 0.5usec), and 320(6.5dBM[fft4] 0.5usec). By inferring the distance using the speed of light at 299,792,458 meters/second the following formula should yield a rough estimate of the distance traveled if a reflection one direction:
$distance_{oneway} = f(x) = 299792458/8000000 * (x - 52) * 0.5 * 3.2$

This first determines the meters traveled per sample at 8MSPS then it multiples that with the number of samples after the suspected TX impulse at sample 13. Then, it is halved by 0.5 since only half that distance was going or coming from the reflecting object which would be the cloud base then that is roughly converted into feet with 3.2.

This gives $f(180) = 7680$, $f(228) = 10560$, $f(288) = 14160$, and $f(320) = 16080$. It is plausible to consider that these represent reflections from the cloud as they are at the appropriate height for clouds in the area at the time; however, it should be noted that the clouds could have been as low as 1000 feet as the humidity and temperature were not acquired and other precise measurements were not possible.

1.2.1 RUN-03

The data is very weak. There are no significant impulses. Perhaps the RX channel started after the TX.

start	length	magnitude	feet
80	500 nsec	5.31dBm[fft4]	1680
100	500 nsec	4.91dBm[fft4]	2880
168	500 nsec	4.47dBm[fft4]	6960
228	500 nsec	6.02dBm[fft4]	10560
272	500 nsec	6.12dBm[fft4]	13200
284	500 nsec	4.77dBm[fft4]	13920
392	500 nsec	6.02dBm[fft4]	20400
868	500 nsec	6.18dBm[fft4]	48960
1412	500 nsec	7.40dBm[fft4]	81600

Table 2: TX-2MSPS-10TICKS.RX-8MSPS-1K6K-30KTICKS-0319161400-RUN05

1.2.2 RUN-04

The data is very weak; however, there are some indications of possible impulses.

1.2.3 RUN-05

The data has strong indications of reflections similar to *RUN-02*.

There is a significant plausible reflection at sample 1412 which indicates a height of 81600 feet or 24km. Some research into the atmosphere has prompted the possibility of the refraction index of air changing at different temperatures, pressures, and water vapor to potentially be reflecting enough of the impulse. An article by Gordon D. Thayer in the journal Radio Science in 1974 gives the following equation to calculate the refractive index[1]: $(n-1)*10^6 = N = 77.6*(P_a/T)*Z_a{}^-1 + 64.8*(e/T)*Z_w{}^-1 + 3.776*10^3*(e/T^2)*Z_w{}^-1$

1.2.4 Conclusion

The confidence in the results of the test is not strong. There appears to be reflections; however, they are difficult to distinguish from various potential sources. It is evident that there exists the potential for cable reflections from impedance mismatches which also include the horn.

2 Session 032316-001

2.1 Internal Reflection Measurement

A primitive measurement of internal reflections from impedance mismatches was devised since hardware was not available to determine this because of expense. A CW sinusoidal of a specific number of samples was produced, transmitted, then the energy at that specific frequency was measured. This was done by rapidly switching the RX channel onto the same antenna port after the TX channel completed operation. See figure 16 in the figures section on page 11. The results showed that there were significantly more energy under and above 3.9GHZ. It is assumed that horns shall have a finite, yet broad, bandwidth, therefore, it is reasonable to assume that the energy is caused by internal reflections. Also, tests show that the angle of radiation is greatly broaded by lower frequencies, therefore, the horn appears to operate effectively at 3.9GHZ which also matches the description located on the LNB+LNA that came with the horn from the satellite TV dish.

2.2 Chirp

The tests from session 031916 on page 2 used a very short transmit time. After, reviewing various materials it was discovered that the reflections may be difficult to determine because they are not very powerful. The idea of increasing pulse length was not originally determined as peak power was supposed to be the primary factor in reflection intensity. This reasoning was found to be incorrect.

The incorrectness is from the ability to accurately detect the reflected pulse. A reflection of 4 samples is extremely difficult to accurately detect as it will be distorted significantly and the weighting of each sample, although high, is insufficient. By reading "'Chirp' A New Radar Technique" by Donald Lancaster published in 1965 in the Electronics World journal it was discovered when Lancaster stated, "Range is determined by the amount of r.f. energy being transmitted. This is equal to the pulse height (power) multiplied by the pulse width (time). (Power X time = energy.) This is equal to the area of the transmitted pulse"[2]. This ground breaking understanding paved the way for understanding the need for an longer pulse duration to overcome the limited peak power of the USRP B200 device without external amplification. Lancaster states:

> To explain chirp, consider the imaginary system of Fig. 1. Instead of transmitting a single frequency pulse, the radar now transmits, in turn, four discrete frequencies forming the over-all transmitted pulse. The first frequency (f1) is transmitted for a time T, then frequency f2 for a time T, then f3 for time T, and finally f4 for time T. The time length T (in microseconds) of each frequency of transmission is identical. The receiver uses four separate filters and detectors for the target-returned frequencies f1, f2, f3, and f4. The outputs of the four detectors are then time-delayed in such a manner that the outputs all "pile up" or coincide in time. Thus, f1 is delayed for 3T seconds, f2 for 2T seconds, f3 for T seconds, and f4 is not delayed. The summed output pulse width is T seconds. However, the original

1. Gordon D. Thayer, "An Improved equation for the radio refractive index of air," *Radio Science*, 10 1974, 803–807, doi:10.1029/RS009i010p00803.

2. Donald Lancaster, ""Chirp" A New Radar Technique," *Electronics World*, January 1965, http://www.rfcafe.com/references/electronics-world/chirp-new-radar-technique-january-1965-electronics-world.htm.

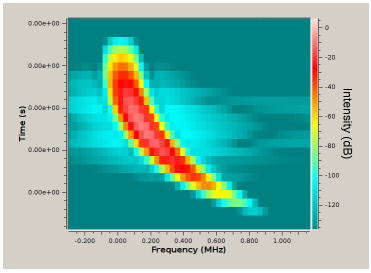

Figure 1: The frequency and time domains of an exponential chirp.

> transmitted pulse was 4T seconds long; therefore, the resolution has been increased by a factor of four with no decrease in transmitted energy. Resolution is determined by what each individual detector receives, which is a pulse only T microseconds wide. With a conventional radar, the return pulse would have to be 4T microseconds wide.

Lancaster's description of the radar chirp changed the approach by modification of the single frequency pulse, current used, into a frequency modulated pulse.

The implementation of the chirp consisted of the code shown in listing 3 in the listing section on page 10. Also, found in the listing section on page 10 as listing 2 is the code to detect the reflected chirps in a sequence of samples of arbitrary length.

2.3 Conclusion

The tests using a chirp did show what appeared to be significant resolution enhancement and increased reflection power levels; however, numerous deviations and strange artefact's existed in the output showing assumed abnormal reflectivity at certain elevations. A review was determined as needed for the chirp detection implementation.

3 Session 032516-001

The chirp detection implementation was reviewed and a mistake identified where the two FIR-like filters for the real and imaginary components had summed the output per sample and squared it. This is believed to have produced abnormal reflectivity by inadequate chirp detection. The implementation was revised and a more rigorous testing via simulation was determined suitable. Also, an exponential chirp was realized as a potential preferred method as detailed by Armin W. Doerry in "Generating Nonlinear FM Chirp Waveforms for Radar" published by Sandia Nationa Laboratories. In this report Doerry explains that the nonlinear chirp has much better characteristics in terms of detection compared to a linearly increasing chirp frequency modulation.

3.1 Tests & Observations

A simulation was devised to simulate noise and a few chirps spread out. The goal is devise the parameters that allow accurate detection of the chirp while being as immune to high level of noise as possible. It would be desired that the chirp would be detectable even under the noise floor. The test is initiated by generating from a fixed random seed a number of samples using a specific uniform noise magnitude. So that each sample consists of a real and imaginary component of the complex number and each component is initialized by multiplying the random value between 0.0 and 1.0 with the noise magnitude. Once generated the chirps would be added to the noise sequence in various potentially overlapping positions.

The chirps were generated using four parameters of *sps*, *base*, *ticks*, and *freq_width* where *sps* is samples per second, *ticks* is the number of samples per chirp, *base* is the base frequency of the chirps, and *freq_width* is the total width in the frequency domain of the chirp. The equation at figure 2 represents the generated of the real and imaginary components per sample s where s is zero-indexed of an array.

$$
\begin{gathered}
s < ticks \\
freq(s) = freq_{base} + (\frac{freq_{width}}{ticks}) * 0.3 * s \\
chirp_{real}(s) = sin(freq(s)) \\
chirp_{imag}(s) = cos(freq(s))
\end{gathered}
$$

Figure 2: The exponential chirp generation equation where s is the zero-indexed offset in the array holding the chirp samples.

$$
\begin{gathered}
s < sps * seconds \\
noise(s) = random() * noise_{mag} \\
noise_{real}(s) = noise(s) \\
noise_{imag}(s) = noise(s)
\end{gathered}
$$

Figure 3: The noise generation for the test sequence of samples.

$$
\sum_{s=offset}^{offset+chirp_{ticks}} final_{real}(s) = noise_{real}(s) + chirp_{real}(s)
$$

$$
\sum_{s=offset}^{offset+chirp_{ticks}} final_{imag}(s) = noise_{imag}(s) + chirp_{imag}(s)
$$

Figure 4: The addition of noise to chirp; however, this is illustrative as the sample sequence was generated with noise and the chirps overlay-ed at potentially random positions.

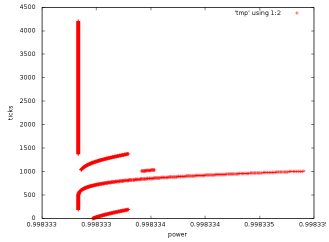

Figure 5: The old chirp detector and filter with linear FM chirp.

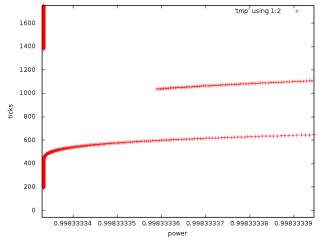

Figure 6: The old chirp detector and filter with linear FM chirp.

The noise was generated as shown in figure 3. The overlay of noise and chirp in figure 4; however, in the actual test the entire sequence has noise generated before overlay of the chirps so that in-between the chirps noise exists.

The test was run with parameters as follows:

sps	48000000
$base$	1000
$ticks$	600
$freq_{width}$	10000
$random_seed$	0
$noise_mag$	0
$time$	1e-4

The old, assumed flawed, chirp filter and detector with a linear chirp produced the result in figure 6. The new chirp filter and detector with an exponential chirp produced the result in figure 7. Oddly, the older chirp filter performed rather well with very sharp edges between chirps on the exponential FM chirp in figure 5

The difference between the new detector and the old is visible when random uniform noise is added. The new detector

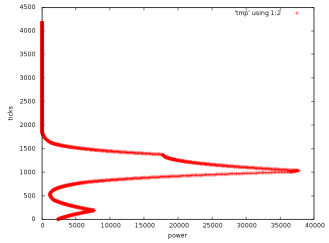

Figure 7: The new chirp detector and filter with exponential FM chirp.

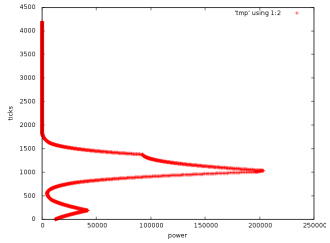

Figure 8: The new chirp detector and filter, exponential FM chirp, and 25dB peak power noise.

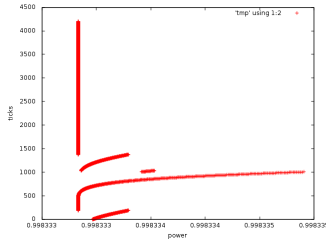

Figure 9: The old chirp detector and filter, exponential FM chirp, and 25dB peak power noise.

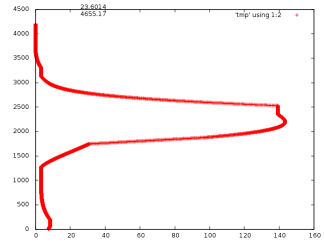

Figure 10: The new chirp detector and filter, exponential FM chirp, 25dB peak power noise, and sinusoidal noise.

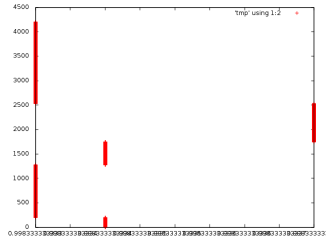

Figure 11: The old chirp detector and filter, exponential FM chirp, 25dB peak power noise, and sinusoidal noise.

is able to reject the noise while the old detector integrates the noise into the power levels; however, unexpected is the ability for the old detector to adequately detect the exponential chirps. The noise peak is 21dB higher than the chirp peak. The old detector is in figure 9 and the new in figure 8. However, impressive the ability of the old detector to perform well it fails to perform under conditions that present non-uniform noise sources or ones that can mimic sinusoidal components by presenting a constant level power for all sample positions while the new detector degrades as shown in figure 11 and 10.

3.2 Conclusion

It is evident that the old chirp detector was inadequate with the linear FM chip and during experimenting it showed some potential in usage with an exponential FM chirp and uniform noise sources; however, it encountered critical failure with strong sinusoidal noise sources. The new detector performed well at the expense of a less sharp edge at the chirps, but it appears to be more reliable and rugged across various types of noise and provides a very low noise floor in its output from uniform noise; however, it was easily degraded by strong sinusoidal noise sources especially if they reside in its chirp bandwidth. It is also beneficial to maximize the chirp bandwidth and in the previous samples this was not done. There is also the difficulty in ensuring that the bandwidth is not so large that it incurs degradation from accuracy issues in signal digital approximation.

The need for a radar emission that meets the criteria for the application is important. It is evident that there is a need for a more robust emission that can survive noise degradation since the current project goal is to establish optimal performance with minimal power.

4 Session 032516-001

The skies were clear except for some very light and barely visible cloud formation. The test had the following parameters:

rx_{sps}	48000000
tx_{sps}	48000000
tx_{gain}	80dB
tx_{active}	True
$tx_{prerxticks}$	500 (Noted mistake; Should be 600)
$tx_{prerxticks_{rate}}$	48000000
tx_{ticks}	600
$freq_{begin}$	3445800000HZ
$gather_{count}$	8000

The noted mistake of 500 may have attributed to some early power levels. The results produced what appeared to be an alternating phase inversion of reflections then a phase inverted elongated reflection and ending with a in-phase small magnitude reflection. This coorelates with METAR reports in the nearby area of a 12000FT cloud ceiling as shown in figure 17 in the figures section on page 12; however, a small image is presented in figure 12 on page 6.

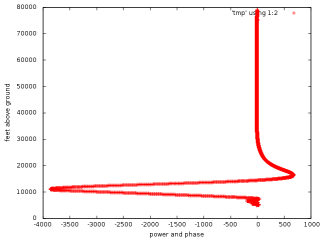

Figure 12: The output from the exponential chirp filter with 450 units of width and 600 ticks at 48MSPS in length for a chirp with RX delayed by 500 samples directed upward at 12dBi to a METAR stated cloud ceiling of 12000FT. See figure 17 in the figures section on page 12 for a full scale image.

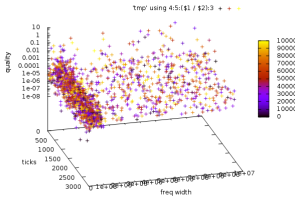

Figure 13: The test data graphed from a number of tests with random parameters comparing the frequency width of the pulse to the pulse length against some static data.

5 Session 032716

A sequence of test data was generated by running one test per a set of parameters. The test consisted of generating uniform noise with the following parameters on each iteration:

Parameter	Lower Bounds	Upper Bounds
sps	48MSPS	48MSPS
$base$	0	100KHZ
$ticks$	0	3000
$freq_{width}$	0	10MHZ
$noise_{mag}$	0.2	0.2

The figure 13 shows the graph of this data. It is evident that there exists large variation in the different parameters and no obvious pattern emerges; however, by sorting the data by quality the following can be arrived at:

quality	base	ticks	$freq_{width}$
2.1515	21.5KHZ	106.665368771	8.1MHZ
0.8274	57.8KHZ	221.113925217	6.3MHZ
0.8269	28.3KHZ	225.721020592	5.8MHZ
0.5424	18.5KHZ	256.352789373	9.3MHZ
0.4815	55.2KHZ	22.9211665375	7.9MHZ
0.4125	3.5KHZ	424.295341219	5.9MHZ
0.3823	57.9KHZ	2.44251047096	3.5MHZ
0.2972	90.6KHZ	263.847380389	7.2MHZ
0.2859	71.1KHZ	96.0395127334	7.1MHZ
0.2293	55.7KHZ	24.4486282096	1.4MHZ
0.2021	32.0KHZ	179.580657555	6.3MHZ
0.1693	7.9KHZ	471.997814279	5.4MHZ
0.1281	44.4KHZ	705.627830587	9.8MHZ
0.1121	22.7KHZ	96.4491960864	7.2MHZ
0.0828	72.0KHZ	1157.64587549	5.4MHZ
0.0758	95.9KHZ	39.1190777886	3.5MHZ
0.0745	52.2KHZ	432.68864096	7.7MHZ
0.0702	98.8KHZ	47.5009599928	1.5MHZ
0.0643	87.4KHZ	159.815303397	7.5MHZ
0.0527	30.9KHZ	331.587149351	762.9KHZ
0.0495	76.3KHZ	77.2093422547	970.3KHZ
0.0492	17.7KHZ	738.50406216	3.0MHZ
0.0487	19.2KHZ	110.443291447	725.0KHZ
0.0483	17.1KHZ	154.550182704	97.6KHZ
0.0463	73.9KHZ	657.060540207	5.2MHZ
0.0420	7.5KHZ	325.219369011	719.3KHZ
0.0378	91.5KHZ	2.70431304614	386.2KHZ
0.0326	68.3KHZ	328.249505268	556.0KHZ
0.0299	16.8KHZ	200.996573013	764.6KHZ
0.0282	62.2KHZ	154.686708333	5.4MHZ
0.0279	51.3KHZ	1026.26449117	9.9MHZ
0.0266	82.9KHZ	1325.47534484	5.3MHZ
0.0255	93.4KHZ	249.353240811	167.6KHZ
0.0251	181.2HZ	1523.91897049	9.5MHZ
0.0193	91.2KHZ	176.648990343	1.7MHZ
0.0169	79.0KHZ	1039.70364719	4.3MHZ
0.0166	42.8KHZ	1719.68668918	3.8MHZ
0.0156	78.7KHZ	352.946355212	3.1MHZ
0.0145	25.5KHZ	627.10241497	927.4KHZ
0.0130	28.9KHZ	926.650457061	4.5MHZ

The simulation was re-run and the uniform noise was eliminated as this would remove the variability of the results. This now showed a different view of the parameters as shown in figure 14 that there is a strong relation visually between the parameters. The relation is that a short pulse length still provides better resolution and the frequency domain width of the pulse is very expensive in terms of compensation if consideration is made to bandwidth.

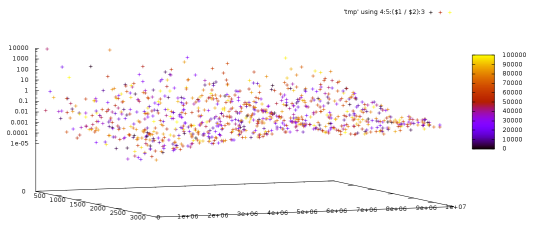

Figure 14: The test data graphed from a number of tests with random parameters comparing the frequency width of the pulse to the pulse length against some static data.

6 Session 032916

6.1 Emission Control

At this point, a working radar system is proven; however, it is not optimal. Yet, despite non-optimality a need exists for assurance before further progression is made.

There is now increased need for reasonable determination of spurious emissions and the checking of output filtering to contain emissions as a secondary precaution and then also rigorous checking to ensure I do not stress those secondary filters. Due to transmits being limited to duration and infrequent assurance can be made that no harmful interference happens and if ever so slightly would be very temporal. Also, my low power output helps ensure that nothing covers great distance at significant power levels.

However, as progression happens into potentially doing more frequent experiments and even during storms the employment of experiments that last a few minutes to a few hours greater verification of spurious and out of band emissions is needed. These including emissions outside the application determined bandwidth, regulatory authority determined bandwidth, and last but not least the actual frequency band of operation as an amateur radio operator. Also, to share the spectrum with other amateurs that may wish to embark on similar experiments that work with a comparable noise floor, thus, making the need for precision measurements of emissions, both intended and unintended, all the more critical.

Work is now progressing on these calculations including developing testing methods and utilization of alternative equipment along with the mathematical reasoning to fully understand the expected emissions of the experiments.

6.2 Findings

```
USRP B200 TX
EVM (error vector magnitude) less than -40dB
TX output uses 128-TAP Finite Impulse Response
```

This was calculated to produce the greatest error of 722CPS using 56MSPS and a 1CPS sinusoidal and at the lowest of roughly 2CPS using various parameters. This gives

reason to include 5KCPS of reasonable buffer bandwidth to experiments.

- test data
  - dump-500-48000000-48000000-48000000-600-3445000000-0-1-5000-0-1-8000-1458933581-mode_rxoffset
- With 1us TX time:
- Energy levels from reflections at
- 20000 feet
- calculated around -200dBW
- Energy level of transmit was 0.1W from transmitter.
- Efficiency of horn antenna was 0.5
- Beam angle was 25 degrees at -3dB
- Transmit time was 12 usecs
- At 31 meters, beam radius was 13 meters.
- At 31 meters, beam wave cross-section area was 3076 sq meters
- At 31 meters, maximum energy density was 0.65uw per 2 sq cm per second.
- Over 166 usecs, peak power from any reflection measured no more than
- ... 1 femto-watt
- Calculations of wave cross-section area after 166usec was estimated to be 1.4 billion square meters with maximum energy density of 30 pico-watts per square meter

6.3 Conclusion

The recorded work showed that safe levels of radio frequency energy are obtained; however, unrecorded results that are to be finished also show that out of application band energy is negligible and out of designated frequency band energy is undetectable. The low-power application also makes wide-band emissions friendly and insignificant to other radio operators.

7 Session 040316

7.1 Aperture Synthesis, Long Distance RX/TX Coherency

The concept of long distance RX/TX with aperture synthesis is not new; however, the design employed under experimentation in amateur radio may be novel. The process would involve a potential test site involving three fixed antennas, of dish type potentially, and secondary antennas providing isotropic radiation for coherency instrumentation.

The fixed dishes would be targeted towards a specific three-dimensional volume as radars and the isotropic antennas would allow coherency building between the sites using a protocol similar to how the Network Time Protocol over the Internet works.

The distance between the fixed dishes may be on the order of thirty nautical miles, thus, providing a relatively large degree of angular accuracy in determining the 3D axis of a reflection, higher resolution, and more accuracy depending on the degree of coherency.

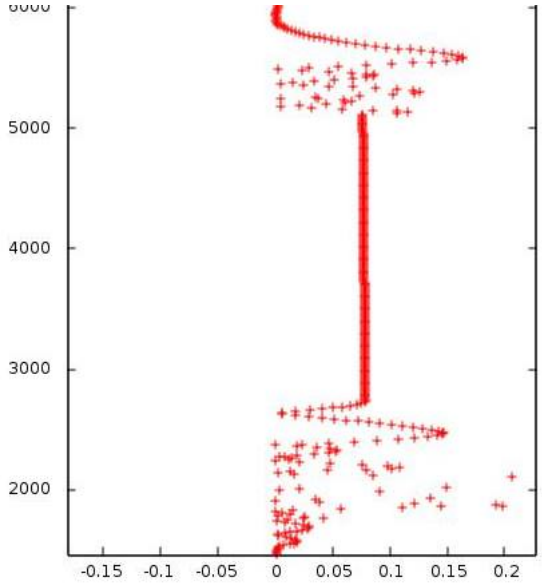

Figure 15: A higher resolution cloud reflection which what may be a double reflection above (reflection from cloud to ground to cloud and back. The data correlates with weather reports of clouds base at the time.

Figure 15 on page 8, shows a higher resolution reflection and if improved and then utilized across multiple sites could provide experimental data.

8 Listings

```
def build_tx_chirp(sps, ticks, freq_width):
out = []
base_freq = 5000.0
freq_step = float(freq_width) / float(ticks)
for x in xrange(0, ticks):
        freq = base_freq + freq_step * float(x)
        d = (float(x) / sps) * freq * math.pi * 2.0
        xx = math.sin(d)
        yy = math.cos(d)
        out.append(xx)
        out.append(yy)
return out
```

Listing 1: The simple code to generate the I/Q samples for a chirp.

```
#
# The frequency offset is hard coded by the 'build_tx_chirp'
# function; however, this is not an optimal design.
#
def compute_reflections(data, sps, chirp_ticks, chirp_spread_factor):
        r = []

        data_real = []
        data_imag = []

        sps = float(sps)
        chirp_ticks = float(chirp_ticks)

    # This happens as all processing is delayed untl after RX
    # and TX. The RX code returns a numpy array and its reference
    # was simply appended to a list. Now, we concatenate them into
    # a single list to simply the following code blocks.
        for z in xrange(0, len(data)):
                for x in xrange(0, len(data[z])):
                        data_real.append(data[z].real[x])
                        data_imag.append(data[z].imag[x])

    # Use the same code that generated the chirp to build the
    # chirp filter.
        chirp = build_tx_chirp(sps, int(chirp_ticks), float(chirp_ticks) * float(chirp_spread_

    # No reflection can be less than this distance since this
    # is the time it takes to transmit the chirp since a single
    # antenna is being used even thought the RX channel does not
    # start until the sample after the last TX sample.
        bmin = (chirp_ticks / sps) * 300000000.0 * 0.5

        reflects = []
        # Potential for testing for phase adjustments or differences.
        for q in xrange(0, 1):
            # Currently not used and equates to zero by (0, 1) above.
                phoff = (math.pi * 2.0) / 8.0 * float(q)
                # This is essentially like a sub-string search algorithm
                # except here we are not looking for a perfect match but
```

```
                # the quality of all matches.
                for x in xrange(0, len(data_real) - (len(chirp) / 2)):
                        p_sum = 0
                    # This is much like a FIR filter. We are evaluating
                    # how well the sampes fit into the mold of the chirp
                    # and recording this result after this loop.
                        for y in xrange(0, len(chirp) / 2):
                                xx = chirp[y*2+0] * data_real[x+y]
                                yy = chirp[y*2+1] * data_imag[x+y]
                                p = math.sqrt(xx ** 2 + yy ** 2)
                                p_sum += p
                        # Normalize p_sum across different chirp lengths
                        # so that test results are easier to interpret and
                        # compare
                        p_sum = p_sum / float(len(chirp))
                        meters = (float(x) / sps) * 300000000.0 * 0.5
                        feet = meters * 3.2
                        # The algorithm is very expensive since it has not
                        # been optimized, therefore, we drop out here; however,
                        # this is simply a preference.
                        if feet > 26000:
                                break
                        reflects.append((p_sum, meters * 3.2 + bmin))
        # There is no need to sort the reflections but sorted order
        # is used for certain checks and tests.
        reflects = sorted(reflects, reverse=True)
        return reflects
```

Listing 2: The inefficient, later determined flawed, but simple code to detect chirp reflections from an arbitrary number of reflections.

```
def build_tx_chirp(sps, ticks, freq_width):
out = []
base_freq = 5000.0
freq_step = float(freq_width) / float(ticks)
for x in xrange(0, ticks):
        freq = base_freq + freq_step * float(x)
        d = (float(x) / sps) * freq * math.pi * 2.0
        xx = math.sin(d)
        yy = math.cos(d)
        out.append(xx)
        out.append(yy)
return out
```

Listing 3: The simple code to generate the I/Q samples for a chirp.

```
#
# The frequency offset is hard coded by the 'build_tx_chirp'
# function; however, this is not an optimal design.
#
def compute_reflections(data, sps, chirp_ticks, chirp_spread_factor):
    # ...
        # ...
            p_sum_x = 0
            p_sum_y = 0
                        for y in xrange(0, len(chirp) / 2):
```

```
                    xx = chirp[y*2+0] * data_real[x+y]
                    yy = chirp[y*2+1] * data_imag[x+y]
                    p_sum_x += xx
                    p_sum_y += yy
                p_sum = p_sum_x * p_sum_y
            # ...
# ...
```

Listing 4: The improved code to detect chirp reflections from an arbitrary number of reflections.

9 Figures

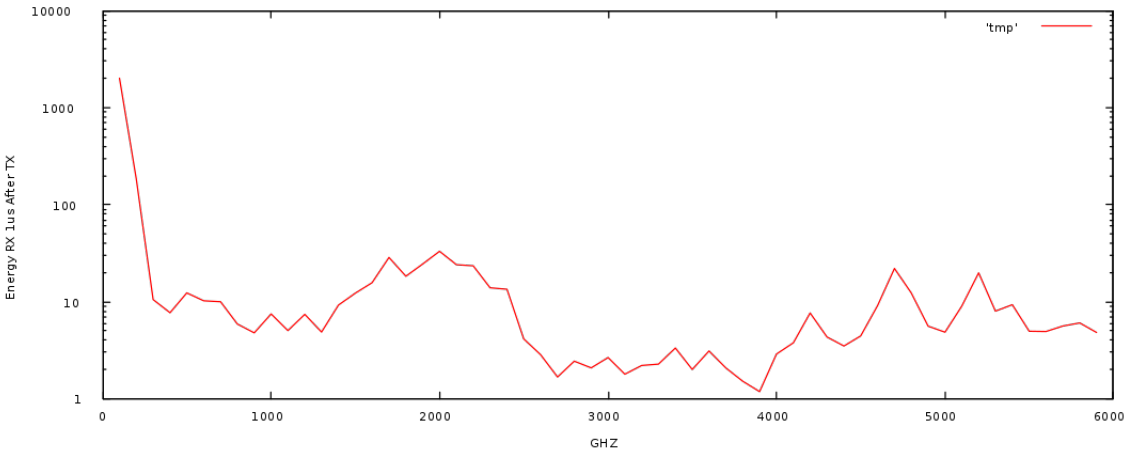

Figure 16: The energy measured at the specific frequency after a 1024 samples at 6MSPS. The horn was directed upwards.

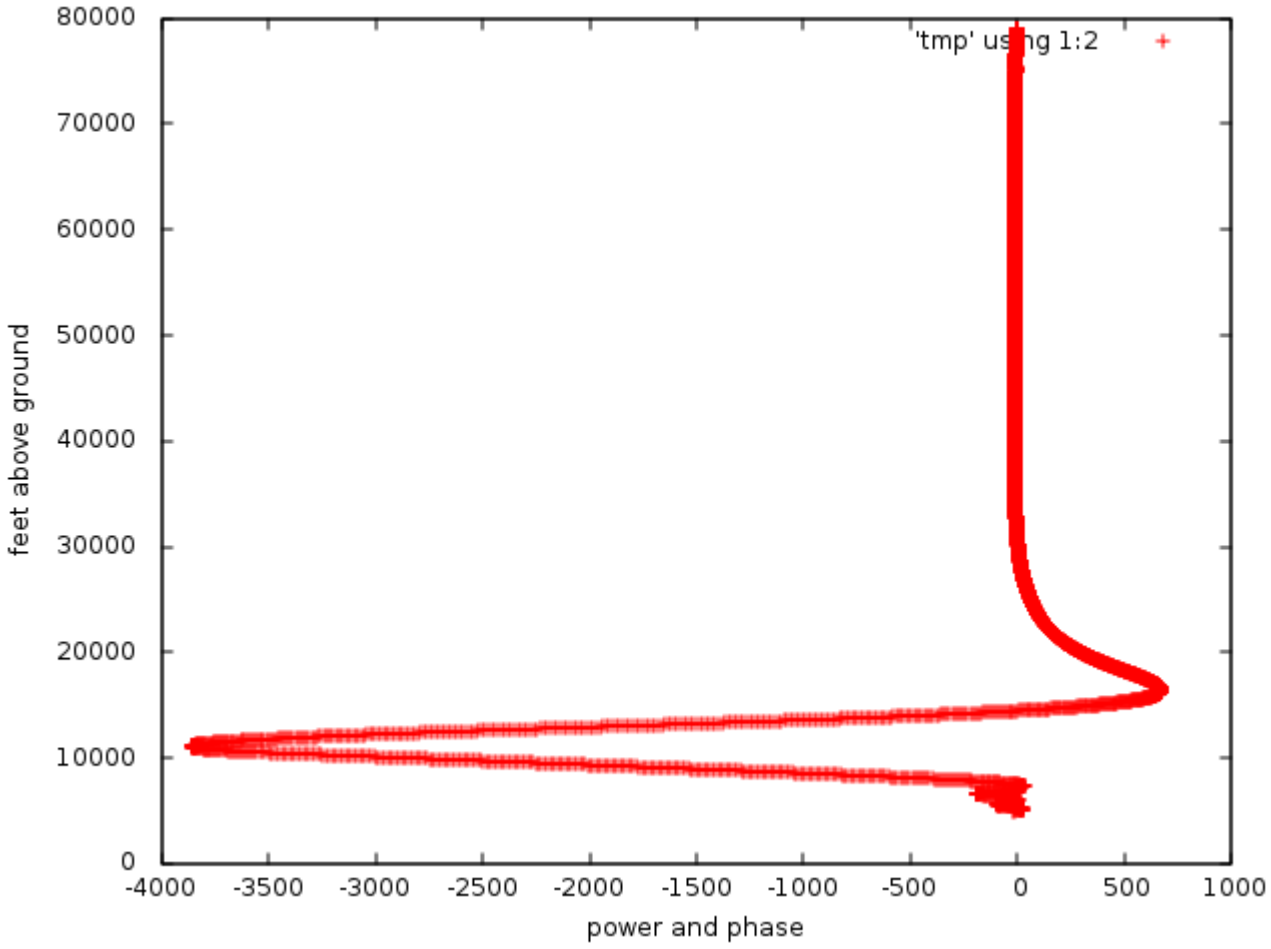

Figure 17: The output from the exponential chirp filter with 450 units of width and 600 ticks at 48MSPS in length for a chirp with RX delayed by 500 samples directed upward at 12dBi to a METAR stated cloud ceiling of 12000FT.

References

Lancaster, Donald. “"Chirp" A New Radar Technique.” *Electronics World*, January 1965. http://www.rfcafe.com/references/electronics-world/chirp-new-radar-technique-january-1965-electronics-world.htm.

Thayer, Gordon D. “An Improved equation for the radio refractive index of air.” *Radio Science*, 10 1974, 803–807. doi:10.1029/RS009i010p00803.